

Towards End-to-End GPS Localization with Neural Pseudorange Correction

Xu Weng, *Student Member, IEEE*, KV Ling, *Member, IEEE*, Haochen Liu, *Student Member, IEEE*, and Kun Cao, *Member, IEEE*

Abstract—Pseudorange errors are the root cause of localization inaccuracy in GPS. Previous data-driven methods regress and eliminate pseudorange errors using handcrafted intermediate labels. Unlike them, we propose an end-to-end GPS localization framework, E2E-PrNet, to train a neural network for pseudorange correction (PrNet) directly using the final task loss calculated with the ground truth of GPS receiver states. The gradients of the loss with respect to learnable parameters are backpropagated through a differentiable nonlinear least squares optimizer to PrNet. The feasibility is verified with GPS data collected by Android phones, showing that E2E-PrNet outperforms the state-of-the-art end-to-end GPS localization methods.

Index Terms—GPS, deep learning, end-to-end learning, localization, pseudoranges, Android phones.

I. INTRODUCTION

PSEUDORANGE errors are a long-standing curse of GPS localization, resulting in positioning errors that are hard to mitigate. Because of their complicated composition, encompassing satellite clock errors, residual atmospheric delays, multipath errors, receiver noise, hardware delays, and so on, how to remove them has long been under active research in the GPS community. Due to the difficulty of modeling pseudorange errors mathematically, researchers have been falling back on big data to attend to this issue.

On the one hand, most previous work performed supervised learning to regress pseudorange errors using handcrafted labels – we only have the ground truth of locations of GPS receivers and have to derive the target values for pseudorange errors using our domain knowledge of GPS. Various derived labels of pseudorange errors are proposed, including pseudorange errors containing residual receiver clock offset [1], double difference of pseudoranges [2], and smoothed pseudorange errors [3]. However, the final task target values – receiver locations – are in place but not used directly. On the other, an end-to-end deep learning approach is proposed to directly map GPS measurements to user locations and implicitly correct pseudorange errors [4]. However, this approach puts considerable but

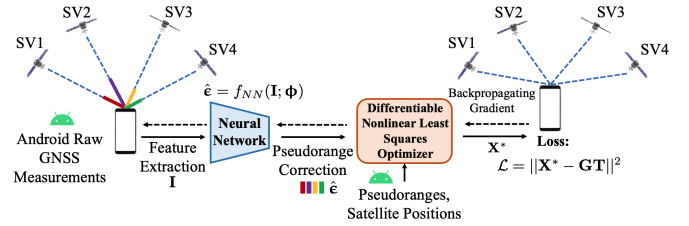


Fig. 1. An overview of our E2E-PrNet GPS localization pipeline. The learnable parameters ϕ of the neural network for pseudorange correction are tuned by the final task loss calculated using the receiver states \mathbf{X}^* .

unnecessary commitment to learning the well-established and robust classical localization theories.

The data-driven methods can learn pseudorange errors while the model-based approaches can perfectly compute locations using the corrected pseudoranges. So, can we combine them so that we can preserve our well-established priors and train the neural modules using the final task loss instead of the intermediate loss? Such hybrid end-to-end pipelines have achieved success in many other domains, including robot control [5], autonomous driving [6], and so on. In the GPS community, recently, an end-to-end learning framework has been proposed to improve GNSS positioning using the differentiable factor graph optimization, the factor weightings of which are tweaked by the final task loss of receiver locations [7].

This paper proposes E2E-PrNet, an end-to-end GPS localization framework with learnable pseudorange correction. As shown in Fig. 1, a neural network (PrNet) is used to regress pseudorange errors that are then combined with other necessary measurements and fed into a Differentiable Nonlinear Least Squares (DNLS) optimizer for location computation. The loss is calculated with the state estimation of the DNLS optimizer and the ground truth of the receiver state, the gradients of which are backpropagated through the DNLS optimizer to tune learnable parameters. To handle the issue that we have no target value for the receiver clock offset, we select its WLS-based estimation as its label. We evaluate our proposed pipeline using Google Smartphone Decimeter Challenge (GSDC) datasets and compare it with the baseline WLS algorithm and the state-of-the-art (SOTA) end-to-end approach. Finally, we explore what the front-end PrNet has learned when trained by the final task loss. The codes of E2E-PrNet are available at <https://github.com/AIlocAR/e2ePrNet>.

X. Weng and K. Ling are with the School of Electrical and Electronic Engineering, Nanyang Technological University, Singapore, 639798, Singapore e-mail: (xu009@e.ntu.edu.sg; ekvling@ntu.edu.sg).

H. Liu is with the School of Mechanical and Aerospace Engineering, Nanyang Technological University, Singapore, 639798, Singapore e-mail: (haochen002@e.ntu.edu.sg).

K. Cao is with the School of Electrical Engineering and Computer Science, KTH Royal Institute of Technology, Stockholm, SE-100 44, Sweden e-mail: (kun001@e.ntu.edu.sg).

Manuscript received April 19, 2005; revised August 26, 2015.

II. PRELIMINARIES OF GPS

To estimate the unknown location $\mathbf{x}_k = [x_k, y_k, z_k]^T$ and the clock offset δt_{u_k} of a GPS receiver at the k^{th} epoch, we need to solve a system of M nonlinear pseudorange equations that measure the distances from the receiver to the M visible satellites. The pseudorange of the n^{th} satellite at the k^{th} epoch can be modeled as

$$\rho_k^{(n)} = \|\mathbf{x}_k - \mathbf{x}_k^{(n)}\| + \delta t_{u_k} + \varepsilon_k^{(n)} \quad (1)$$

where $\mathbf{x}_k^{(n)}$ denotes the satellite position. $\varepsilon_k^{(n)}$ is the measurement error, which includes the multipath/NLOS delays, residual atmospheric delays, hardware delays, measurement noise, etc. The measurement error can be considered as the sum of the denoised pseudorange error $\mu_k^{(n)}$ and unbiased pseudorange noise $v_k^{(n)}$, i.e., $\varepsilon_k^{(n)} = \mu_k^{(n)} + v_k^{(n)}$. With an approximation to the receiver's state $\tilde{\mathbf{X}}_k = [\tilde{x}_k, \tilde{y}_k, \tilde{z}_k, \delta \tilde{t}_{u_k}]^T$, we can apply the Gauss-Newton algorithm to calculate the least squares (LS) estimation of the receiver's state $\hat{\mathbf{X}}_k = [\hat{x}_k, \hat{y}_k, \hat{z}_k, \delta \hat{t}_{u_k}]^T$:

$$\mathbf{X}_k = \tilde{\mathbf{X}}_k - (\mathbf{J}_{\mathbf{r}_k}^T \mathbf{J}_{\mathbf{r}_k})^{-1} \mathbf{J}_{\mathbf{r}_k}^T \mathbf{r}(\tilde{\mathbf{X}}_k) \quad (2)$$

where

$$\begin{aligned} \mathbf{r}(\tilde{\mathbf{X}}_k) &= [\tilde{r}_k^{(1)}, \tilde{r}_k^{(2)}, \dots, \tilde{r}_k^{(M)}]^T \\ \tilde{r}_k^{(n)} &= \rho_k^{(n)} - \|\tilde{\mathbf{x}}_k - \mathbf{x}_k^{(n)}\| - \delta \tilde{t}_{u_k} \\ \mathbf{J}_{\mathbf{r}_k} &= \left[\frac{\partial \tilde{r}_k^{(i)}}{\partial X_j}(\tilde{\mathbf{X}}_k) \right]_{M \times 4} \end{aligned}$$

We run (2) iteratively until a certain criterion is fulfilled. Let $\mathbf{H}_k = (\mathbf{J}_{\mathbf{r}_k}^T \mathbf{J}_{\mathbf{r}_k})^{-1} \mathbf{J}_{\mathbf{r}_k}^T$ and $\hat{\mathbf{X}}_k$ represent the state estimation. We assume \mathbf{H}_k has been weighted implicitly using pseudorange uncertainty. Then, the weighted least squares (WLS) estimation error $\varepsilon_{\mathbf{X}_k}$ is:

$$\varepsilon_{\mathbf{X}_k} = \mathbf{X}_k - \hat{\mathbf{X}}_k = -\mathbf{H}_k \varepsilon_k \quad (3)$$

where ε_k is the pseudorange error vector of visible satellites.

III. METHODOLOGY

As (3) shows, a key to improving GPS localization accuracy is to reduce the pseudorange measurement errors. To this end, we propose an end-to-end learning pipeline (E2E-PrNet) to train a neural network for pseudorange correction using the final task loss of GPS. As shown in Fig. 1, we connect the neural network output to a DNLS optimizer for state estimation. The loss is calculated with the estimated and true receiver state, and its gradients are backpropagated through the DNLS optimizer to the neural network to tune the learnable parameters.

A. Neural Pseudorange Correction

We employ PrNet as the neural network for correcting pseudoranges considering its SOTA performance [3]. PrNet was proposed to regress the pseudorange errors from six satellite, receiver, and context-related input features:

$$\hat{\varepsilon}_k^{(n)} = f_{NN}(\mathbf{I}_k^{(n)}; \Phi)$$

where $\mathbf{I}_k^{(n)}$ represents the input features for the n^{th} satellite. Φ is the vector of learnable parameters of the neural network. As a paradigm of supervised learning, target values of pseudorange errors are manually derived from the receiver location ground truth as follows [3].

$$\mu_k^{(n)} - \mathbf{h}_{t_k}^T \mathbf{M}_k = \|\bar{\mathbf{x}}_k - \mathbf{x}_k^{(n)}\| - \|\mathbf{x}_k - \mathbf{x}_k^{(n)}\| \quad (4)$$

where $\mathbf{h}_{t_k}^T$ is the last row vector of the matrix \mathbf{H}_k . The vector \mathbf{M}_k represents the denoised pseudorange errors of all visible satellites, i.e., $\mathbf{M}_k = [\mu_k^{(1)}, \mu_k^{(2)}, \dots, \mu_k^{(M)}]^T$. $\bar{\mathbf{x}}_k$ is the smoothed estimation of the receiver location. Note that the common delay item $-\mathbf{h}_{t_k}^T \mathbf{M}_k$ for all visible satellites does not affect the localization accuracy.

B. Differentiable Nonlinear Least Squares Optimizer

We consider GPS localization as a nonlinear least squares optimization problem:

$$\mathbf{X}_k^* = \min_{\mathbf{X}_k} \frac{1}{2} \|\mathbf{r}_k(\mathbf{X}_k)\|^2 \quad (5)$$

where

$$\begin{aligned} \mathbf{r}(\mathbf{X}_k) &= [r_k^{(1)}, r_k^{(2)}, \dots, r_k^{(M)}]^T \\ r_k^{(n)} &= \rho_k^{(n)} - \hat{\varepsilon}_k^{(n)} - \|\mathbf{x}_k - \mathbf{x}_k^{(n)}\| - \delta t_{u_k} \end{aligned} \quad (6)$$

The optimization variables include the receiver's location and clock offset, i.e., $\mathbf{X}_k = [x_k, y_k, z_k, \delta t_{u_k}]^T$. The auxiliary variables are satellite locations $[\mathbf{x}_k^{(n)}]_M$, pseudorange measurements $[\rho_k^{(n)}]_M$, and neural pseudorange corrections $\hat{\varepsilon}_k = [\hat{\varepsilon}_k^{(n)}]_M$. The data-driven module and the model-based module are connected via (6). Then, the final task loss is computed with the optimized and true receiver state \mathbf{X}_k :

$$\mathcal{L} = \|\mathbf{X}_k^* - \mathbf{X}_k\|^2.$$

The derivative of the loss function with respect to the learnable parameters Φ of the front-end neural network is calculated as

$$\frac{\partial \mathcal{L}}{\partial \Phi} = \frac{\partial \mathcal{L}}{\partial \mathbf{X}_k^*} \cdot \frac{\partial \mathbf{X}_k^*}{\partial \hat{\varepsilon}_k} \cdot \frac{\partial \hat{\varepsilon}_k}{\partial \Phi} \quad (7)$$

where the first derivative of the right side of (7) is easy to compute considering its explicit form. The last one can be solved in a standard training process. But computing the derivative of the optimal state estimation \mathbf{X}_k^* with respect to the neural pseudorange correction $\hat{\varepsilon}_k$ is challenging due to the differentiation through the nonlinear least squares problem. We use Theseus, a generic DNLS library, to solve the optimization problem (5) and calculate the derivative (7) since it provides various algorithms to backpropagate gradients like (7) [8].

C. Handling the Missing Label Issue

In practice, we can collect the ground truth of user locations using high-performance geodetic GPS receivers integrated with other kinds of sensors, such as visual-inertial localization systems. The ground truth of receiver clock offset, however, is difficult to obtain. We choose the WLS-based estimation of the receiver clock offset $\delta \hat{t}_{u_k}$ as the target value of δt_{u_k} :

$$\delta \hat{t}_{u_k} = \delta t_{u_k} + \mathbf{h}_{t_k}^T \varepsilon_k \quad (8)$$

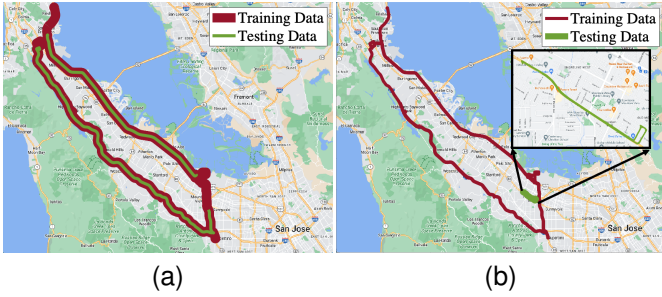


Fig. 2. (a) Scenario I: fingerprinting. (b) Scenario II: cross trace.

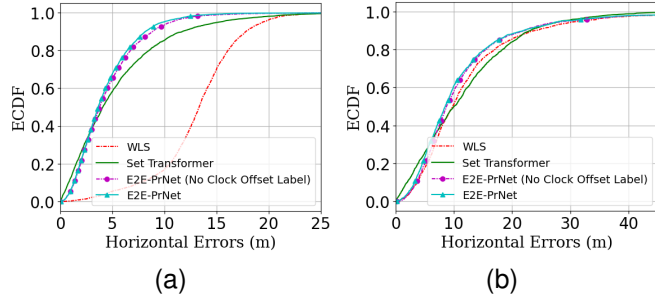


Fig. 3. ECDF of horizontal errors in (a) Scenario I. (b) Scenario II.

Considering a perfectly trained E2E-PrNet, i.e., its output is the exactly same as the ground truth, we can get the following equations according to (1), (5), (6), and (8).

$$\begin{aligned}\hat{\varepsilon}_k^{(n)} &= \varepsilon_k^{(n)} - \mathbf{h}_{t_k}^T \boldsymbol{\varepsilon}_k \\ &= \mu_k^{(n)} - \mathbf{h}_{t_k}^T \mathbf{M}_k + v_k^{(n)} - \mathbf{h}_{t_k}^T \boldsymbol{\Upsilon}_k\end{aligned}\quad (9)$$

where $\boldsymbol{\Upsilon}_k = [v_k^{(1)}, v_k^{(2)}, \dots, v_k^{(M)}]^T$ is the unbiased pseudorange noise of all visible satellites. Therefore, by comparing (4) and (9), we can conclude that the proposed E2E-PrNet is equivalent to a PrNet trained with noisy pseudorange errors.

IV. EXPERIMENTS

A. Datasets and Implementations

1) *Datasets*: To evaluate E2E-PrNet, we employ the open dataset of Android raw GNSS measurements for Google Smartphone Decimeter Challenge (GSDC) 2021 [9]. After removing the degenerate data, we select twelve traces for training and two traces for inference, all of which are collected on highways. As shown in Fig. 2, we design two localization scenarios – fingerprinting and cross trace – to investigate our prospect that a model pre-trained in an area can be distributed to users in the exact area to improve GPS localization.

2) *Implementations of E2E-PrNet*: We use Pytorch, d2l, and Theseus [8] libraries to implement our proposed E2E-PrNet. The neural network module in the end-to-end framework is implemented as a multilayer perceptron with 20 hidden layers and 40 neurons in each layer, according to [3]. About the configuration of Theseus, we use a Gauss-Newton optimizer with a step size of 0.5 and 50 loop iterations. The optimizer uses a dense Cholesky solver for forward computation and backpropagates gradients in the unroll mode.

TABLE I
HORIZONTAL POSITIONING SCORES OF END-TO-END SOLUTIONS

Methods	Horizontal Score (meter)↓	
	Scenario I	Scenario II
WLS	16.390	20.666
Set Transformer	9.699 ($\mu = 15\text{m}$)	19.247 ($\mu = 22\text{m}$)
E2E-PrNet (No RCOL)	7.239	19.158
E2E-PrNet	6.777	18.520

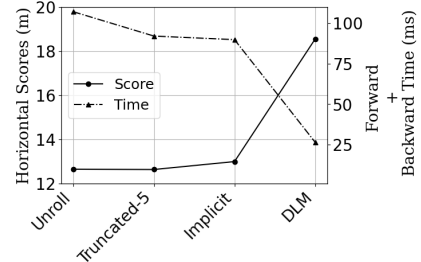


Fig. 4. Backward mode analysis for configuring Theseus.

To validate our strategy for dealing with missing receiver clock offset labels (RCOL), we also train an E2E-PrNet using location ground truth only.

3) *Implementations of Baseline Methods*: We choose the WLS method as the baseline model-based method and implement it according to [10]. We also compare our proposed framework with set transformer, an open source SOTA end-to-end deep learning approach to improve positioning performance over Android raw GNSS measurements [4]. We set the key argument in set transformer – the magnitude of initialization ranges μ – according to the 95th percentile of the 3D localization errors of the WLS method. The weights of our trained set transformer are available at https://github.com/ailocar/deep_gnss/data/weights/RouteR_e2e.

B. Horizontal Errors

The horizontal error is the key indicator of GPS positioning performance in our daily applications. Google employs the horizontal scores calculated with Vincenty’s formulae as the official metric to compare localization solutions in GSDC. We give the empirical cumulative distribution function (ECDF) of horizontal errors of our proposed E2E-PrNet and the baseline methods in Fig. 3 and summarize their horizontal scores in Table I. Among the end-to-end localization methods, our proposed E2E-PrNet obtains the best horizontal positioning performance in the two scenarios, with its ECDF curves generally being on the left side of those of other solutions. Quantitatively, E2E-PrNet achieves 59% and 10% improvement in horizontal scores compared to WLS. And its scores are also smaller than the set transformer by 30% and 4%. Compared with E2E-PrNet trained without RCOL, E2E-PrNet trained with the WLS-based estimation of receiver clock offset obtains better horizontal positioning performance.

C. Discussion on Backward Modes

Theseus designs four backward modes for training, including unrolling differentiation, truncated differentiation, implicit

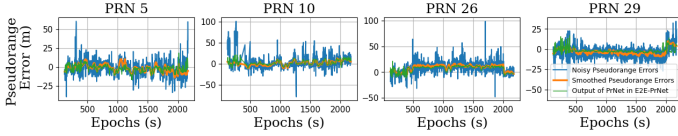


Fig. 5. Output of the front-end PrNet in the E2E-PrNet framework.

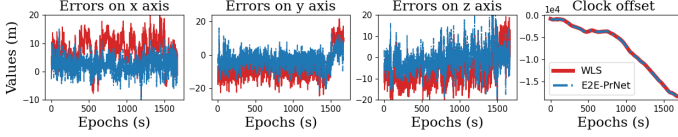


Fig. 6. State estimations of WLS and E2E-PrNet.

differentiation, and direct loss minimization (DLM). Their training performance varies across different applications [8]. Thus, we compare them in terms of the training time and the final horizontal localization scores during inference, as shown in Fig. 4. It indicates that the unroll mode, truncated-5, and implicit modes share similar inference accuracy. The latter two modes have shorter training time than the basic unroll mode because they have shorter backpropagation steps. DLM obtains the fastest training speed but the largest horizontal errors. And we need to carefully tune the hyperparameters of DLM to keep its horizontal score small.

D. Discussion on Explainability

To verify whether the front-end PrNet in E2E-PrNet behaves as we expected, we log down its output data during inference – the input to the downstream DNLS optimizer – and draw them together with the noisy and smoothed pseudorange errors in Fig. 5. Here, we only draw the results of four satellites, and the other visible satellites share a similar phenomenon. While (9) indicates the front-end PrNet should be trained under noisy pseudorange errors, Fig. 5 shows it approximately learns the smoothed pseudorange errors. This phenomenon can be explained by the observations that deep neural networks are robust to and can learn information from noisy training labels [11]. Then, the output of the front-end PrNet is approximately

$$\hat{\varepsilon}_k^{(n)} = \mu_k^{(n)} - \mathbf{h}_{t_k}^T \mathbf{M}_k. \quad (10)$$

Submitting (1) and (10) into (6) and letting (6) be zero yield

$$\|\mathbf{x}_k - \mathbf{x}_k^{(n)}\| + (\delta t_{u_k} - \mathbf{h}_{t_k}^T \mathbf{M}_k) = \rho_{c_k}^{(n)} + v_k$$

where $\rho_{c_k}^{(n)} = \rho_k^{(n)} - \varepsilon_k^{(n)}$ is the clean pseudorange with its measurement error removed. According to (3), the state estimation is

$$\hat{x}_k = x_k + \mathbf{h}_{x_k}^T \boldsymbol{\Upsilon}_k, \hat{y}_k = y_k + \mathbf{h}_{y_k}^T \boldsymbol{\Upsilon}_k, \hat{z}_k = z_k + \mathbf{h}_{z_k}^T \boldsymbol{\Upsilon}_k, \\ \delta \hat{t}_{u_k} = \delta t_{u_k} + \mathbf{h}_{t_k}^T \boldsymbol{\varepsilon}_k$$

where $\mathbf{h}_{x_k}^T$, $\mathbf{h}_{y_k}^T$, and $\mathbf{h}_{z_k}^T$ are the 1st-3rd row vectors of \mathbf{H}_k . Thus, the final output states should be approximately the WLS-based location estimation with biased errors removed and the WLS-based clock offset estimation, which is verified by Fig. 6. We also compare the horizontal localization of E2E-PrNet

 TABLE II
 COMPARISON BETWEEN E2E-PRNET AND PRNET

Methods	Horizontal Score (meter) ↓	
	Scenario I	Scenario II
E2E-PrNet	6.777	18.520
PrNet+Noisy Labels	6.922	18.434
PrNet+Smoothed Labels	6.537	19.524

with that of PrNets trained with noisy and smoothed labels, as displayed in Table II, which shows similar horizontal scores and is aligned with our analysis that E2E-PrNet nearly learns the smoothed pseudorange errors.

V. CONCLUSION

This paper explores the feasibility of training a neural network to correct GPS pseudoranges using the final task loss. To this end, we propose E2E-PrNet, an end-to-end GPS localization framework composed of a PrNet and a DNLS module. Our experiments on GSDC datasets showcase its superiority over the classical WLS method and the SOTA end-to-end method. E2E-PrNet benefits from PrNet's superior ability to correct pseudoranges while mapping raw data directly to locations. In the future, we will integrate the classical filtering algorithms into E2E-PrNet for noise suppression and study its feasibility in urban canyons with weak signal strength.

REFERENCES

- [1] Rui Sun, Guanyu Wang, Qi Cheng, Linxia Fu, Kai-Wei Chiang, Li-Ta Hsu, and Washington Yotto Ochieng. Improving GPS code phase positioning accuracy in urban environments using machine learning. *IEEE Internet of Things Journal*, 8(8):7065–7078, 2020.
- [2] Guohao Zhang, Penghui Xu, Haosheng Xu, and Li-Ta Hsu. Prediction on the urban GNSS measurement uncertainty based on deep learning networks with long short-term memory. *IEEE Sensors Journal*, 21(18):20563–20577, 2021.
- [3] Xu Weng, Keck Voon Ling, and Haochen Liu. PrNet: A neural network for correcting pseudoranges to improve positioning with android raw GNSS measurements. *arXiv preprint arXiv:2309.12204*, 2023.
- [4] Ashwin V Kanhere, Shubh Gupta, Akshay Shetty, and Grace Gao. Improving GNSS positioning using neural-network-based corrections. *NAVIGATION: Journal of the Institute of Navigation*, 69(4), 2022.
- [5] Bingheng Wang, Zhengtian Ma, Shupeng Lai, and Lin Zhao. Neural moving horizon estimation for robust flight control. *IEEE Transactions on Robotics*, 2023.
- [6] Zhiyu Huang, Haochen Liu, Jingda Wu, and Chen Lv. Differentiable integrated motion prediction and planning with learnable cost function for autonomous driving. *IEEE Transactions on Neural Networks and Learning Systems*, 2023.
- [7] Penghui Xu, Hoi-Fung Ng, Yihan Zhong, Guohao Zhang, Weisong Wen, Bo Yang, and Li-Ta Hsu. Differentiable factor graph optimization with intelligent covariance adaptation for accurate smartphone positioning. In *Proceedings of the 36th International Technical Meeting of the Satellite Division of The Institute of Navigation*, pages 2765–2773, 2023.
- [8] Luis Pineda, Taosha Fan, Maurizio Monge, Shobha Venkataraman, Paloma Sodhi, Ricky TQ Chen, Joseph Ortiz, Daniel DeTone, Austin Wang, Stuart Anderson, et al. Theseus: A library for differentiable nonlinear optimization. *Advances in Neural Information Processing Systems*, 35:3801–3818, 2022.
- [9] Guoyu Michael Fu, Mohammed Khider, and Frank van Diggelen. Android raw GNSS measurement datasets for precise positioning. In *Proceedings of the 33rd international technical meeting of the satellite division of the Institute of Navigation*, pages 1925–1937, 2020.
- [10] Xu Weng and Keck Voon Ling. Localization with noisy android raw gnss measurements. In *2023 IEEE Asia Pacific Conference on Wireless and Mobile (APWiMob)*, pages 95–101. IEEE, 2023.
- [11] David Rolnick, Andreas Veit, Serge Belongie, and Nir Shavit. Deep learning is robust to massive label noise. *arXiv preprint arXiv:1705.10694*, 2017.